

# On possibility of synthesizing superheavy elements in nuclear explosions

Alexander Botvina<sup>a,b</sup>, Igor Mishustin<sup>a,c</sup>, Valery Zagrebaev<sup>a,d</sup> and  
Walter Greiner<sup>a</sup>

<sup>a</sup>*Frankfurt Institute for Advanced Studies, J.W. Goethe University, D-60438 Frankfurt  
am Main, Germany*

<sup>b</sup>*Institute for Nuclear Research, Russian Academy of Sciences, 117312 Moscow, Russia*

<sup>c</sup>*Kurchatov Institute, Russian Research Center, 123182 Moscow, Russia*

<sup>d</sup>*Joint Institute for Nuclear Research, 141980 Dubna, Russia*

## Abstract

The possibility to produce superheavy elements in the course of low-yield nuclear explosions is analyzed within a simple kinetic model which includes neutron capture,  $\gamma$ -emission, fission and particle evaporation from excited nuclei. We have calculated average numbers of absorbed neutrons as well as mass distributions of U and Cm nuclei exposed to an impulsive neutron flux as functions of its duration. It is demonstrated that detectable amounts of heavy nuclei absorbing from 20 to 60 neutrons may be produced in this process. According to an optimistic scenario, after multiple  $\beta$ -decay such nuclei may reach the long-living elements of the predicted “island of stability”.

PACS: 26.30.-k, 28.70.+y, 27.90.+b, 28.20.Fc

## 1. Introduction

Synthesis of new elements is one of the main goals of nuclear physics during the last century. First elements heavier than uranium were synthesized in nuclear reactors via neutron-capture reactions followed by  $\beta$ -decay. These reactions were efficient enough to produce elements up to  $Z=100$  (Fm). Nuclei with larger  $Z$  are produced with accelerator-based experiments, most often via the fusion reaction involving  $\alpha$ -particles and heavy ions. In heavy-ion induced fusion reactions new nuclei up to  $Z=118$  were synthesized during the last decades [1, 2, 3]. However, the nuclei produced in the cold fusion reactions [1, 2] are situated just along the proton drip-line, thus being very neutron-deficient and short-lived. Fusion of actinides with  $^{48}\text{Ca}$  leads to more neutron-rich superheavy nuclei with longer half-lives [3]. However, they are still far from the predicted “island of stability”, where the expected life times of even neutron-richer isotopes should be much longer [4]. Indeed, life times of newly synthesized heavy elements with  $Z = 108\text{--}118$ , increase with increasing neutron content [3]. This is consistent with theoretical predictions of the island of stability at the neutron number  $N\approx 184$  and proton numbers around  $Z=114$ ,  $Z=120$ ,

and eventually also  $Z=126$ . Even more neutron-rich nuclei could be produced in multi-nucleon transfer processes in low-energy collisions of heavy actinide nuclei like  $U+Cm$  [5]. However, the cross sections of such processes are rather low.

In this paper we discuss another possibility for synthesizing heavy and superheavy elements which should be more appropriate for obtaining neutron-rich nuclei up to their drip-lines. Namely, we propose to use intensive neutron fluxes generated by nuclear explosions. Actually, this method was already partially employed alongside with nuclear reactors in the 60-s [6, 7]. However, because of some technical and political constraints it was abandoned later. Nevertheless, this method provides the highest neutron densities which are not possible to reach with other terrestrial techniques.

Our general ideas are illustrated in Fig. 1. It shows the upper end of the nuclear chart with the hypothetical “island of stability”. The typical fusion reactions like  $^{238}U + ^{48}Ca$  lead to proton-rich compound nuclei which lie above the  $\beta$ -stability line. On the other hand, the multiple neutron-capture reactions in nuclear explosions may bring the  $^{238}U$  nuclei to the neutron drip-line. Then, after the neutron flux ceased, these nuclei undergo multiple  $\beta$ -decay and come close to the island of stability from the neutron-rich side. If a single explosion is insufficient, then, in principle, a properly delayed second explosion can do the job.

Several underground explosions carried out by scientists at the Livermore and Los Alamos Laboratories were dedicated to synthesizing new elements [6, 7, 8]. They include Par (1964), Barbel (1964), Tweed (1965), Vulcan (1966), and Cyclamen (1966). The elements up to  $^{257}Fm$  were found in explosion debris by radiochemical methods. From published descriptions of these experiments one can conclude that little special effort was made to increase the neutron flux and irradiation time for target nuclei as compared with standard explosions. Also it is unlikely that the debris material, which was extracted for the analysis, was located near the central zone characterized by the most intensive neutron exposure [9]. Although the experimental equipment available at that time was not very sophisticated, it was sufficient to demonstrate the high efficiency of this method by observing the absorption of up to 20 neutrons by the U target. As discussed in refs. [8, 10] more heavy elements might have been produced, but they might decay via spontaneous fission avoiding detection with radiochemical methods. These results were discussed in the review article by Glenn Seaborg [6] with the conclusion that even higher-mass nuclei may be produced in explosions, if the neutron exposures were increased, and special targets were used.

As will be demonstrated below, the multiple neutron absorption by heavy nuclei in the course of a nuclear explosion can lead to very high mass numbers close to the neutron drip-line. Not only a few but macroscopic amounts of such neutron-rich heavy and super-heavy nuclei may be produced in this way. Studying these processes may lead to better understanding of nucleosynthesis in r-processes associated with supernova explosions. We believe that some open questions of cosmic nucleosynthesis can be tested in nuclear explosion experiments by using special target materials and detection techniques. In our estimates below we use only open publications and Internet resources regarding the characteristics of explosive devices.

## 2. Main physical processes contributing to explosive nucleosynthesis.

For our calculations we adopt a very simple model of the active zone associated with a low-yield nuclear explosion [11]. We assume that it can be represented as a medium consisting of fissioning nuclei, fission products, light charged particles, neutrons, and photons. This medium is characterized by a certain temperature  $T$  which has typical values of  $5 \div 10$  keV at the pre-expansion stage. Then we consider the time evolution of mass and charge distributions of nuclear species by taking into account all possible reactions with surrounding particles and subsequent decays. Elastic neutron collisions with nuclei, which do not change mass and charge distributions, are not considered here. It is assumed that after each inelastic interaction the nucleus relaxes to a new equilibrium state (compound nucleus). In particular, the  $(n, \gamma)$  reaction is considered as a two-step process, including the neutron absorption at the first step and the photon emission at the second step. Specifically, in our analysis we include the following processes:

*Absorption of particles by a nucleus.* The neutron capture by the nucleus with mass number  $A$  is characterized by the width

$$\Gamma_n^{cap} = \hbar \langle v_{rel} \sigma_n \rangle \rho_n. \quad (1)$$

Here  $v_{rel}$  is relative  $nA$  velocity which is close to the thermal neutron velocity  $v_n = \sqrt{(3T/m_N)}$  (in units  $c$ ,  $m_N = 939$  MeV, mass of nucleon),  $\rho_n$  is the density of neutrons. For the neutron capture cross section  $\sigma_n$  we take the inelastic part of the  $nA$  cross section, i.e.  $\sigma_n = \sigma_{tot} - \sigma_{el}$ . The corresponding evaluated data were taken from the web site [12]. Our analysis shows that in the neutron energy range between 2 MeV and 10 keV these cross sections may change by several times. Also, they show a considerable odd-even effect as functions of mass. For U isotopes the changes are between 1.5 barn for odd isotopes and 0.3 barn for even isotopes. For Cm isotopes the corresponding changes are between 3 barn and 0.5 barn. For our rough estimates below we take  $\sigma_n=1$  barn for U and 2 barn for Cm, independent of neutron energy and mass number of the nucleus.

At relatively low temperatures considered here the cross-sections for capturing free protons and light charged clusters like  $\alpha$ -particles are negligible. However, in thermonuclear explosions the 14 MeV neutrons from the fusion reaction ( $d + t \rightarrow {}^4\text{He} + n$ ) may transfer energy to  $d$  and  $t$  nuclei, sufficient to induce  $(d, \gamma)$ ,  $(t, \gamma)$  and other reactions [10], which we do not consider here.

The capture of a photon by the nucleus is characterized by the width

$$\Gamma_\gamma^{cap} = \hbar \langle v_\gamma \sigma_\gamma(E_\gamma) \rangle \rho_\gamma. \quad (2)$$

Here  $E_\gamma = T(\pi^4/(30 \cdot 1.202)) \approx 2.7T$  is the average energy of photons in matter,  $v_\gamma \approx c$  is the in-medium velocity of photons, and the density of photons is given by

$$\rho_\gamma = \frac{2 \cdot 1.202}{\pi^2} \frac{T^3}{(c\hbar)^3}. \quad (3)$$

*Emission of particles from the nucleus.* The width for evaporation of a particle  $j$  ( $j = n, p, d, t, {}^3\text{He}, \alpha$ ) from the compound nucleus  $(A, Z)$  is given by:

$$\Gamma_j = \int_0^{E_{AZ}^* - B_j} \frac{\mu_j g_j^{(i)}}{\pi^2 \hbar^2} \sigma_j(E) \frac{\rho_{A'Z'}(E_{AZ}^* - B_j - E)}{\rho_{AZ}(E_{AZ}^*)} E dE. \quad (4)$$

Here  $\rho_{AZ}$  and  $\rho_{A'Z'}$  are the level densities of the initial  $(A, Z)$  and final  $(A', Z')$  compound nuclei,  $E_{AZ}^*$  is the excitation energy of the initial nucleus,  $E$  is the kinetic energy of an emitted particle,  $g_j = (2s_j + 1)$  is its spin degeneracy factor,  $\mu_j$  and  $B_j$  stand, respectively, for the reduced mass and separation energy of the ejectile. The cross section  $\sigma_j(E)$  of the inverse reaction  $(A', Z') + j = (A, Z)$  is calculated using the optical model with corresponding nucleus-nucleus potential [13]. The evaporation process was simulated by the Monte Carlo method and the conservation of energy and momentum was strictly controlled at each emission step.

In the particular case of photon evaporation from an excited nucleus the corresponding width is given by [14]

$$\Gamma_\gamma = \int_0^{E_{AZ}^*} \frac{E^2}{\pi^2 c^2 \hbar^2} \sigma_\gamma(E) \frac{\rho_{AZ}(E_{AZ}^* - E)}{\rho_{AZ}(E_{AZ}^*)} dE, \quad (5)$$

where  $E$  is the photon energy. The integration is performed numerically. Within the dipole approximation the photo-absorption cross section is expressed as:

$$\sigma_\gamma(E) = \frac{\sigma_0 E^2 \Gamma_R^2}{(E^2 - E_R^2)^2 + \Gamma_R^2 E^2}. \quad (6)$$

Here the empirical parameters of the giant dipole resonance have the values  $\sigma_0 = 2.5A$  mb,  $\Gamma_R = 0.3E_R$ , and  $E_R = 40.3/A^{1/5}$  MeV. In the situation which we consider here the photon energies are in the range from about 4 MeV to 100 keV, i.e. considerably smaller than the resonance energy,  $E_R \approx 13.4$  MeV for  $A = 250$ . Thus, the photo-absorption cross section is rather small,  $\sigma_\gamma < 0.01\sigma_0$ .

Fission is an important de-excitation channel for heavy nuclei ( $A > 200$ ), which can compete with particle emission. It is also included in the Monte-Carlo simulations. Following the Bohr-Wheeler statistical approach we assume that the partial width for the fission of compound nucleus is proportional to the level density  $\rho_{sp}$  at the saddle point of the fission barrier [15]:

$$\Gamma_f = \frac{1}{2\pi \rho_{AZ}(E_{AZ}^*)} \int_0^{E_{AZ}^* - B_f} \rho_{sp}(E_{AZ}^* - B_f - E) dE, \quad (7)$$

where  $B_f$  is the height of the fission barrier which is determined according to the Myers-Swiatecki prescription [16]. For  $\rho_{sp}$  we have used approximations obtained in ref. [14] from the extensive analysis of nuclear fissility and  $\Gamma_n/\Gamma_f$  branching ratios.

*Beta-decay.* There are many approaches to such a complicated problem as  $\beta$ -decay. In our calculations we are mostly dealing with nuclei far from the  $\beta$  stability region.

Their masses and  $\beta$ -decay rates have significant uncertainties. On the other hand, it is well known that  $\beta$ -decay is rather slow in comparison with other nuclear processes, it has characteristic times of milliseconds and more. A maximum effect of  $\beta$ -decay was estimated by taking the rates for 'allowed' transitions from the Sargent diagram [17]. In particular, we have used the following interpolation of the decay rate  $\lambda$  (in 1/sec):

$$\log(\lambda) = 4\log(E_{max}) - 3, \quad (8)$$

where  $E_{max}$  (in MeV) is the maximum energy of emitted electrons, assuming that the daughter nucleus is in its ground state. Then the corresponding decay width is  $\Gamma_{\beta} = \hbar\lambda$ . For nuclei in the vicinity of the drip-line this formula predicts life times of order of milliseconds [18].

*Spontaneous fission and  $\alpha$ -decay.* Spontaneous fission is characterized by even longer times than  $\beta$ -decay. It will certainly affect the yield of superheavy elements before extraction of a sample for analysis. However, it has practically no influence on the accumulation of neutrons by the target nucleus. To take into account this process we have employed a simple parametrization of the fission half-lives proposed in ref. [8]. Typical half-lives for alpha-decay of these neutron-rich nuclei are usually longer than years and this decay mode can be completely ignored in the calculations.

### 3. Physical conditions in the active zone

*Neutron density:* For our further calculations we should know the density of neutrons generated in the active zone of an explosion. Let us assume a 100 kt explosion which corresponds to fissioning of  $1.45 \cdot 10^{25}$  nuclei of  $^{235}\text{U}$  (or  $^{239}\text{Pu}$ ) with total mass of 5.6 kg. At normal density this amount of U or Pu has the volume of about  $300 \text{ cm}^3$ . Assuming that about 1.3 new neutrons are produced in average per fission, we can estimate the total number of free neutrons to be  $2 \cdot 10^{25}$ . This gives the maximum neutron density of about  $6 \cdot 10^{22} \text{ cm}^{-3}$ . However, due to a finite efficiency, the amount of the fissile material and accordingly its volume should be larger. On the other hand, with the implosion assembly method, the fissile material is initially compressed by several times, that will increase accordingly the neutron density. According to ref. [11], the neutron multiplication process should be over within the time interval of about  $1.5 \cdot 10^{-7}$  sec after beginning of the chain reaction. To this time the density of free neutrons increases exponentially and reaches the maximum values estimated above. Many of these fission neutrons may leave the core. However, some of them might be reflected back with an appropriate reflector to keep the neutron density in the core higher. These neutrons have a chance to slow down to thermal energies corresponding to temperatures  $T \approx 10 \text{ keV}$  at the early expansion stage. Taking into account all these uncertainties as well as strong time dependence of the neutron yield, in our estimates below we use several values for the neutron density, from  $4 \cdot 10^{22} \text{ cm}^{-3}$  to  $4 \cdot 10^{20} \text{ cm}^{-3}$ .

One can also consider a thermonuclear reaction as a source of additional fast neutrons in combined fission-fusion set-ups. We have found that the neutron densities at the end of

the fusion stage are rather similar to the values estimated above. However, the subsequent evolution of the neutron density will be different in these two cases, because of a very different composition of the active zone.

*Characteristic time scales:* There are several important time scales which influence strongly the efficiency of the neutron capture reaction. Obviously, the goal is to maximize the time  $\tau$  of the target exposure to the strongest neutron flux. The shortest time scale is the neutron multiplication time  $\tau_m$  associated with the chain reaction. This time is determined by the properties of the fissile material and is typically in the range of 0.1  $\mu\text{sec}$ , as mentioned above. Such short times are obtained when all available neutrons are used for fission reactions, to maximize the yield of the explosion. However, this time will increase significantly if the active zone would contain more nuclei absorbing neutrons, like  $^{238}\text{U}$  (reduced enrichment), bringing the system closer to the critical regime.

The disassembly stage is defined by a condition that the chain reaction is ceased. This happens when most of the fission energy is deposited in the active zone and the matter is transformed into a radiation-dominated hot and dense plasma. Due to the huge internal pressure it would rapidly expand into the vacuum, if nothing is done to confine it. However, by introducing a heavy tamper around the active zone, one can delay the fast expansion of plasma to a few microseconds. This time is needed for the shock wave to propagate through the thick layer of heavy tamper's material, usually  $^{238}\text{U}$ . The hydrodynamic time can be estimated as a time required for the rarefaction wave to reach the center of the active zone,  $\tau_h \approx R/c_s \lesssim 10\mu\text{sec}$ , where  $R$  is the core radius and  $c_s$  is the sound velocity in the core. The tamper can also serve as a reflector and absorber for the neutrons. To explore the whole parameter space, in our calculations we consider the exposure times  $\tau$  from 0.1 to 3  $\mu\text{sec}$ .

Another important time scale is the neutron thermalization time  $\tau_{th}$  in the medium. If the medium consists mostly of heavy nuclei like U, the neutron energy loss is dominated by inelastic collisions with these nuclei, followed by the photon emission from the excited nuclei. For slowing down the fission neutrons to thermal velocities  $v_n(T)$  several ( $\sim 10$ ) such collisions are needed. Therefore, we can estimate thermalization time as  $\tau_{th} \sim 10\lambda/v_n$ , where  $\lambda$  is the neutron mean free path (few cm). Then one obtains  $\tau_{th} \sim 1\mu\text{sec}$ , which is usually shorter than the hydrodynamic time.

#### 4. Synthesis of nuclei by multiple neutron capture

*Evolution of average mass number:* We have performed calculations for the  $^{238}\text{U}$  and  $^{248}\text{Cm}$  target nuclei embedded in the active zone of the explosion for several fixed values of neutron density  $\rho_n$  and temperature  $T$ . The  $^{238}\text{U}$  nuclei are usually present in the explosive devices in the fissile material or in a tamper, but  $^{248}\text{Cm}$  nuclei can be additionally installed in the core.<sup>1</sup> Instead of solving a complicated set of rate equations for the ensemble of different nuclear species, we first consider the fate of one individual target nucleus in this environment. We start at  $t=0$  with a nucleus  $A$  in the ground state and consider all

---

<sup>1</sup>The Cm isotopes are produced in significant quantities in nuclear reactors, and they have a sufficient lifetime to be used as a target for the neutron irradiation.

processes which can change its mass number or excitation energy. At each time step we evaluate the probabilities of these processes,  $p_j = \Gamma_j / (\sum_k \Gamma_k)$ , in accordance with the rates  $\Gamma_j$  discussed in the previous section. Then we choose the reaction by the Monte Carlo method and change accordingly the state of the nucleus. If process  $j$  is chosen, the clock is changed by time interval  $\Delta t = \hbar/\Gamma_j$ . This method allows us to follow the stochastic evolution of an "average" nucleus.

The average mass numbers of U and Cm isotopes are shown in Fig. 2 as functions of time. The dotted lines show the calculations for fast fission neutrons (mean kinetic energy of 1.5 MeV) assuming no moderation at all. The other lines show the results for thermalized neutrons at temperature  $T=10$  keV and several neutron densities. Due to a higher flux, the fast neutrons dominate at early times,  $t < 0.3 \mu\text{sec}$ . However during this time interval the target nuclei can absorb only a few neutrons. The efficient nucleosynthesis may proceed only at longer times, when the neutrons have already slowed down. Then, due to the lower excitation energy, the probability of channels with re-emission of neutrons from the compound nucleus is strongly reduced as compared with reactions induced by MeV-neutrons. This is why with increasing  $A$  the absorption rate becomes higher for keV-neutrons. The calculations show that a considerable part of curium (more than 90%) undergoes fission in reactions with fast neutrons. However, in the case of thermalized neutrons this channel is less probable and the majority of nuclei (nearly 95%) survive. One can see from the figure that U and Cm nuclei can in average absorb 10-15 neutrons during the time interval of 1  $\mu\text{sec}$ , if the neutron density remains high,  $4 \cdot 10^{22} \text{ cm}^{-3}$  or higher. Since the neutron capture process has a stochastic character, even much larger numbers of neutrons could be accumulated with certain probabilities (see the next subsection).

The main mechanism of increasing the nuclear mass number works as following. A neutron captured by a nucleus with mass  $A$  brings a few MeV excitation to the new nucleus  $A+1$ . This excitation energy is only slightly above the neutron separation energy, which is expected to decrease with the neutron excess. It is typically below the fission barrier, especially in neutron-rich isotopes. The probability to return a neutron in the evaporation process is also low because of the small phase space volume of the final state. In this situation  $\gamma$ -emission is the main decay mechanism for reducing the excitation energy. After the first photon carries away some energy, the next  $\gamma$ -emissions become even more probable in comparison with other decay channels. This continues until the excitation is decreased nearly to zero, and then the relative probability to capture a new neutron becomes high again. With fixed  $Z$  and increasing  $A$  the fission probability decreases, since the fissility parameter  $Z^2/A$  becomes lower. In the time interval  $\lesssim 1$  msec the  $\beta$ -decay still has a very low probability in order to compete with other processes. In the long run the survival of produced superheavy nuclei will depend on whether they can avoid spontaneous fission and  $\alpha$ -decay in order to reach the island of stability via multiple  $\beta$ -decays.

As our calculations show, the outcome of explosive nucleosynthesis depends crucially on the masses and level densities of nuclei far away from the  $\beta$ -stability line. There are no experimental data in this region, and theoretical models often give controversial results.

Our previous calculations were performed with Myers-Swiiatecki (MS) mass formula [16]. The predictions based on the Cameron mass formula [19] are shown in Fig. 3 for U and Cm targets too. In principal, if the neutron flux remains high the capture of neutrons may continue until the target nucleus reaches the neutron drip-line. Then the probability of neutron emission increases considerably, and, in the case of U, it dominates over the photon emission. The “dynamical” equilibrium between absorption and emission of neutrons at the drip-line depends weakly on the neutron density and may last for a long time (more than milliseconds) until the  $\beta$ -decay makes the  $Z+1$  nucleus. As the result, the drip-line is shifted to the right and absorption of neutrons becomes possible again, of course, if the neutron density remains high enough. One can see that the Cameron formula leads to similar results for U and Cm nuclei, with saturation at large  $A$ . However, the MS formula predicts slightly different Cm masses around  $A \approx 280$  as compared to the Cameron formula. This leads to a smaller ratio of the neutron and photon evaporation widths,  $\Gamma_n/\Gamma_\gamma$ , so that the emission of photons is more probable in the MS case. This gives a chance to absorb more neutrons in Cm target, contrary to the U target, and, finally, enter the mass region with more bound neutrons.

*Calculation of nuclear abundances:* For practical applications, it is very important to estimate the amount of new isotopes produced by this mechanism. In Figs. 2 and 3 we have presented the evolution of an average mass number of the target nucleus, ignoring the distribution around the average. This analysis has provided us with better understanding of the main mechanisms responsible for increasing the nuclear mass number under various external conditions. As turned out, at temperatures  $T \sim 10$  keV we can simply consider a capture of neutrons followed by the emission of photons, without complications induced by re-emission of neutrons and fission. In this case we can write the set of coupled equations for densities of nuclei with mass numbers  $A=A_0, A_0+1, A_0+2, \dots$  :

$$\begin{aligned} \frac{d\rho_{A_0}}{dt} &= -\langle v_{rel}\sigma_n \rangle \rho_n \rho_{A_0}, \\ \frac{d\rho_{A+1}}{dt} &= \langle v_{rel}\sigma_n \rangle \rho_n \rho_A - \langle v_{rel}\sigma_n \rangle \rho_n \rho_{A+1}, \end{aligned} \quad (9)$$

which can be solved numerically for any given time dependence of the neutron density  $\rho_n$ . Here  $v_{rel}$  is the neutron-nucleus relative velocity which is close to the neutron velocity  $v_n$ , and  $\sigma_n$  is the neutron capture cross-section (see section 2), which is assumed here to be independent of the nuclide mass number.<sup>2</sup> These equations describe the evolution of the ensemble of nuclear species due to the neutron capture reactions with gain ( $A-1 \rightarrow A$ ) and loss ( $A \rightarrow A+1$ ) terms. It is worth noting that final nuclide abundances depend only on the time-integrated neutron flux  $\Phi = \int \rho_n v_n dt \approx v_n \rho_n \tau$ . According to the analysis of refs. [7, 8, 10], typical values of  $\Phi$  reached in low-yield nuclear explosions are in the range of  $3 \cdot 10^{24} \div 10^{25} \text{ n/cm}^2$ .

---

<sup>2</sup> Of course, when the neutron number approaches the drip-line limit, the capture cross section  $\sigma_n$  will strongly decrease, and the solution of the equations will be more complicated.



In Fig. 4 we present the distributions of isotope abundances after exposure of a  $^{238}\text{U}$  target to a constant neutron flux during fixed time intervals indicated at the lines. The figure shows that the distribution of neutron-rich isotopes becomes broader with increasing the exposure time, or, equivalently, the integrated neutron flux  $\Phi$ . According to refs. [7, 10], in samples of material extracted from underground explosion sites concentrations of rare nuclei ( $A=257$ ) on the level of  $10^{-11} - 10^{-12}$  were measured by radiochemical methods. Even higher sensitivity can be reached by using mass spectroscopic methods (see, e.g., [20]). In typical nuclear explosions mentioned above the observed neutron-rich isotopes have not more than 20 absorbed neutrons [7, 10]. According to calculations of Fig. 4, where neutron density was fixed at  $4 \cdot 10^{22} \text{ cm}^{-3}$ , to produce such isotopes in observable amounts we would need  $\tau \approx 0.3 \mu\text{sec}$ . This corresponds to the integrated neutron flux of about  $2 \cdot 10^{24} \text{ n/cm}^2$ , which within a factor of 2 agrees with the values estimated in refs. [7, 10].

From Fig. 4 we conclude that observable concentrations of nuclei with more than 40 absorbed neutrons can be obtained only if the exposure time is longer than  $1 \mu\text{sec}$ . Obviously, to increase the number of captured neutrons one should increase the integrated neutron flux  $\Phi$ , i.e. either by increasing the neutron density  $\rho_n$  or by increasing the exposure time  $\tau$ .<sup>3</sup> To achieve this goal one can try e.g. to increase the neutron multiplication time by introducing neutron absorbers, reflectors, and other construction elements. With the exposure time of  $3 \mu\text{sec}$  the fraction of nuclei captured 50 neutrons would be about  $10^{-8}$ . In this case, even if we take 1 gram of the exotic target material like  $^{248}\text{Cm}$ , the concentration of nuclides with  $A \approx 300$  will be  $10^{-12}$  which could be detected by present experimental methods.

These results suggest that the drip-line region can in principle be reached in a properly optimized explosive processes. Obviously, new experiments are required to explore this region. They should not only be limited to searching for long-lived superheavy elements, where the yield may be essentially affected by spontaneous fission. Heavy and intermediate-mass nuclei in the vicinity of their neutron drip-lines could be synthesized in this way too. For example, we have found that under the same conditions a Pb nucleus may capture nearly 40 neutrons and come close to the drip-line. This approach to the drip-line has an important advantage as compared with heavy-ion reactions, because nuclei enter this region with minimal excitation energy. However, due to expected short live-times of these nuclei, their properties can only be studied by analyzing their decay products.

## 5. Conclusions

It is obvious that the nuclear explosions provide the highest fluxes of neutrons under terrestrial conditions which will hardly be feasible with any other experimental technique. We have demonstrated that irradiation of nuclei with neutrons produced during the first microseconds of a nuclear explosion is a very promising way to synthesize neutron-rich

---

<sup>3</sup>We are taking here about time scales which are still much less than the  $\beta$ -decay times, i.e. milliseconds.

heavy and super-heavy elements. For comparison, modern spallation sources (e.g. ESS) may supply thermal neutrons with densities around  $10^{12} \text{ cm}^{-3}$ , and nuclear reactors – with  $10^{11} \text{ cm}^{-3}$  [21]. We believe, there exist technical possibilities to increase the time and intensity of target exposure in the course of a nuclear explosion. They may include preliminary compression of fissile material, introducing neutron reflectors and moderators, as well as special construction of targets. The main idea of optimization should be to maximize the neutron density and exposure time and to minimize the energy yield of the explosion. Another possibility which should be considered in more details is generating two or several nuclear explosions within a time delay up to milliseconds in close proximity of each other. This delay may be sufficient for very neutron-rich nuclei produced in the first explosion to undergo multiple  $\beta$ -decay. Then the daughter nuclei will be able to absorb additional neutrons from the second explosion, and in this way increase the resulting mass number, as illustrated in Fig. 1. Even mass production of super-heavy elements can be envisaged in the future.

The methods discussed above can be used not only for synthesizing long-living super-heavy elements but also for production of very neutron-rich isotopes in the vicinity of the drip-line. These studies are extremely important for understanding the origin of heavy elements in the Universe. Hot and dense environments created in nuclear explosions are rather similar to conditions in supernova explosions, when heavy nuclei are produced by multiple neutron capture in  $r$ -process.

If long-lived superheavy elements are indeed produced in the explosions, an important question to be answered is, how to find them among tons of debris. In underground explosions the processed material may be extracted and analysed by radio-chemical and mass-spectroscopic methods. Generally, the methods used for searching for superheavy elements in nature [22] may be applied in this case too.

The authors thank Yu. Ts. Oganessian, I. Pshenichnov and S. Schramm for fruitful discussions. A.B. acknowledges the financial support received from the Helmholtz International Center for FAIR within the framework of the LOEWE program (Landesoffensive zur Entwicklung Wissenschaftlich-Okonomischer Exzellenz) launched by the State of Hesse. This work was supported in part by the grants NS-7235.2010.2 and RFBR 09-02-91331 (Russia).

## References

- [1] S. Hofmann and G. Munzenberg, *Rev. Mod. Phys.* **72**, 733 (2000).
- [2] K. Morita et al., *J. Phys. Soc. Jpn.* **76**, No. 4, 045001 (2007).
- [3] Yu.Ts. Oganessian, V. K. Utyonkov et al., *Phys. Rev. C* **74**, 044602 (2006).
- [4] U. Mosel and W. Greiner, *Z. Phys.* **222**, 261 (1969). J. Grumann, U. Mosel, B. Fink, and W. Greiner, *Z. Phys.* **228**, 371 (1969).
- [5] Valery Zagrebaev and Walter Greiner, *Phys. Rev. C* **78**, 034610 (2008).

- [6] G.T. Seaborg, *Ann. Rev. Nucl. Sci.* **18**, 119 (1968).
- [7] A.S. Krivochatsky, Yu.F. Romanov, Production of transuranium and actinide elements by neutron irradiation (in Russian), 320 p., Atomizdat, Moscow, 1969.
- [8] George I. Bell, *Phys. Rev.* **158**, 1127 (1967).
- [9] Combined Radiochemistry Group, *Phys. Rev.* **148**, 1192 (1966).
- [10] George I. Bell, *Phys. Rev.* **139**, B 1207 (1965).
- [11] H.A. Sandmeier, S.A. Dupree, G.E. Hansen, *Nucl. Sci. Eng.* **48**, 343 (1972).
- [12] <http://www-nds.iaea.org/exfor/endl.htm>
- [13] A.S. Botvina, A.S. Iljinov, I.N. Mishustin, J.P. Bondorf, R. Donangelo, K. Sneppen, *Nucl. Phys. A* **475**, 663 (1987).
- [14] A.S. Iljinov, M.V. Mebel, N. Bianchi, E. De Sanctis, C. Guaraldo, V. Lucherini, V. Muccifora, E. Polli, A.R. Reolon, P. Rossi, *Nucl. Phys.* **A543**, 517 (1992).
- [15] J.P. Bondorf, A.S. Botvina, A.S. Iljinov, I.N. Mishustin and K. Sneppen, *Phys. Rep.* **257**, 133 (1995).
- [16] W.D. Myers and W.J. Swiatecki, *Nucl. Phys. A* **81**, 1 (1966).
- [17] N. Feather and H.O.W. Richardson, *Proc. Phys. Soc.* **61**, 452 (1948). J.K. Major and L.C. Biedenharn, *Rev. Mod. Phys.* **26**, 321 (1954).
- [18] P. Moeller, J.R. Nix, K.-L. Kratz, *At. Data Nucl. Data Tables* **66** 131 (1997).
- [19] A.G.W. Cameron, *Can. J. Phys.* **35**, 1021 (1957).
- [20] F. Dellinger, O. Forstner, R. Golser, W. Kutschera, A. Priller, P. Steier, A. Wallner, G. Winkler, *Nucl. Instr. Meth. B* **268**, 1287 (2010).
- [21] see, e.g., <http://www.ess-neutrons.eu>
- [22] G.N. Flerov and G.M. Ter-Akopian, *Rep. Prog. Phys.* **46**, 817 (1983). J. McMinn, H.R. Ihle, R. Wagner, *Nucl. Instr. Meth.* **139**, 175 (1976). W. Stephens, J. Klein, R.Zurmuehle, *Phys. Rev. C* **21**, 1664 (1980).

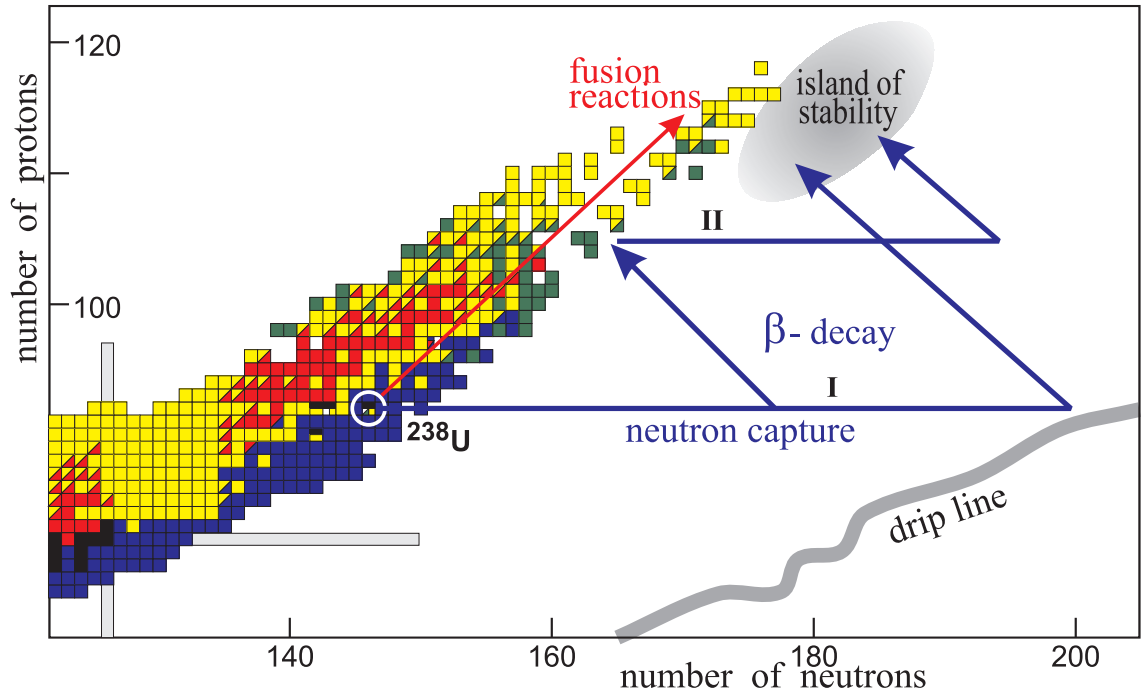


Figure 1: (Colour online) The upper end of the nuclear chart showing the experimentally investigated isotopes. The colours stand for the decay modes: yellow -  $\alpha$ -decay, red -  $\beta^+$  or electron capture, blue -  $\beta^-$  decay, green - spontaneous fission. Black boxes are stable nuclei. Grey area is the predicted “island of stability”. Red arrow represents the heavy-ion fusion reactions used so far. Blue arrows show schematically the proposed explosion-based methods to reach this island: I indicates fast capture of neutrons during first microseconds of the nuclear explosion followed by the  $\beta$ -decay. II indicates second nuclear explosion within few milliseconds after the first one.

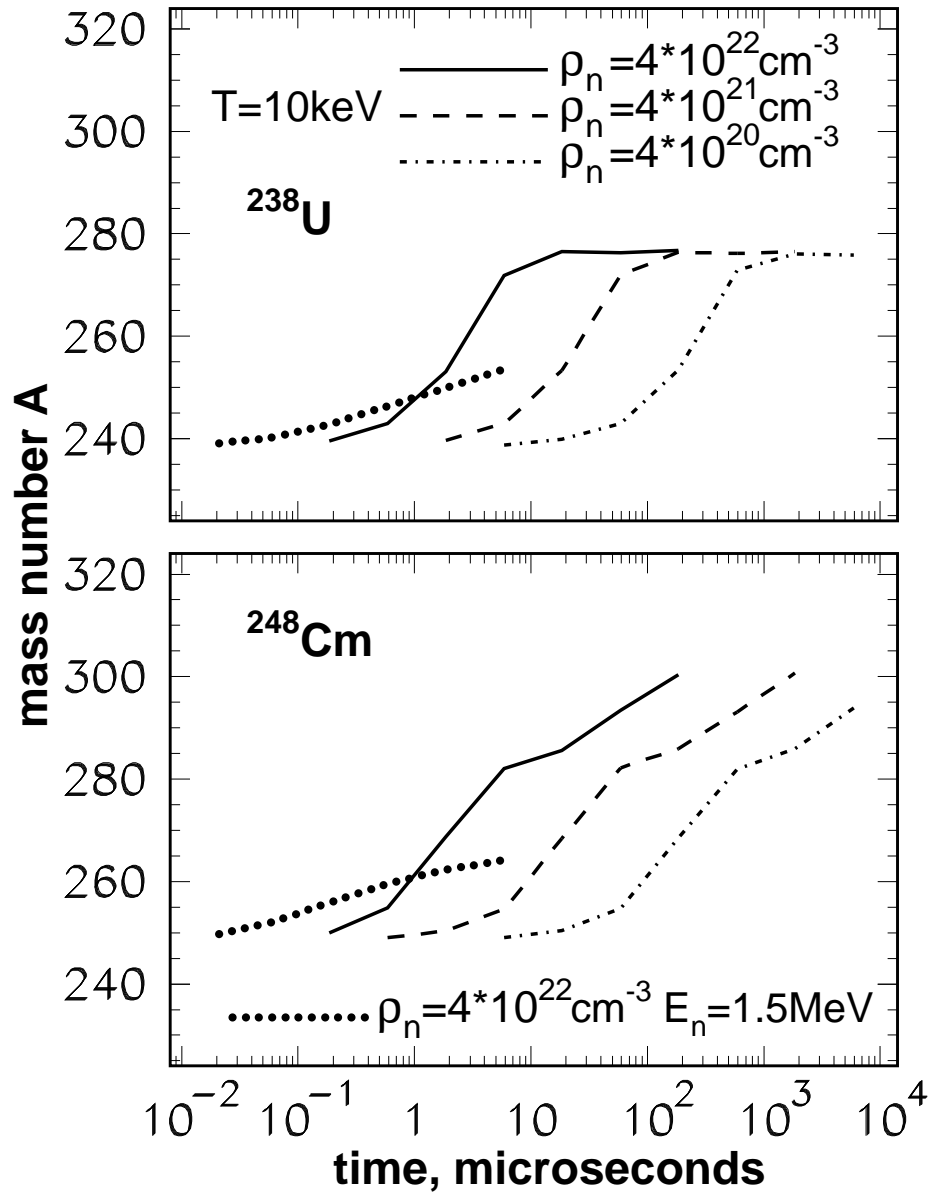


Figure 2: Evolution of U (top panel) and Cm (bottom panel) mass numbers with time at the neutron densities shown at the figure. (The initial target nuclei are  $^{238}\text{U}$  and  $^{248}\text{Cm}$ .) Dotted line presents absorption of fast neutrons, other lines - absorption of thermalized neutrons at  $T=10 \text{keV}$ .

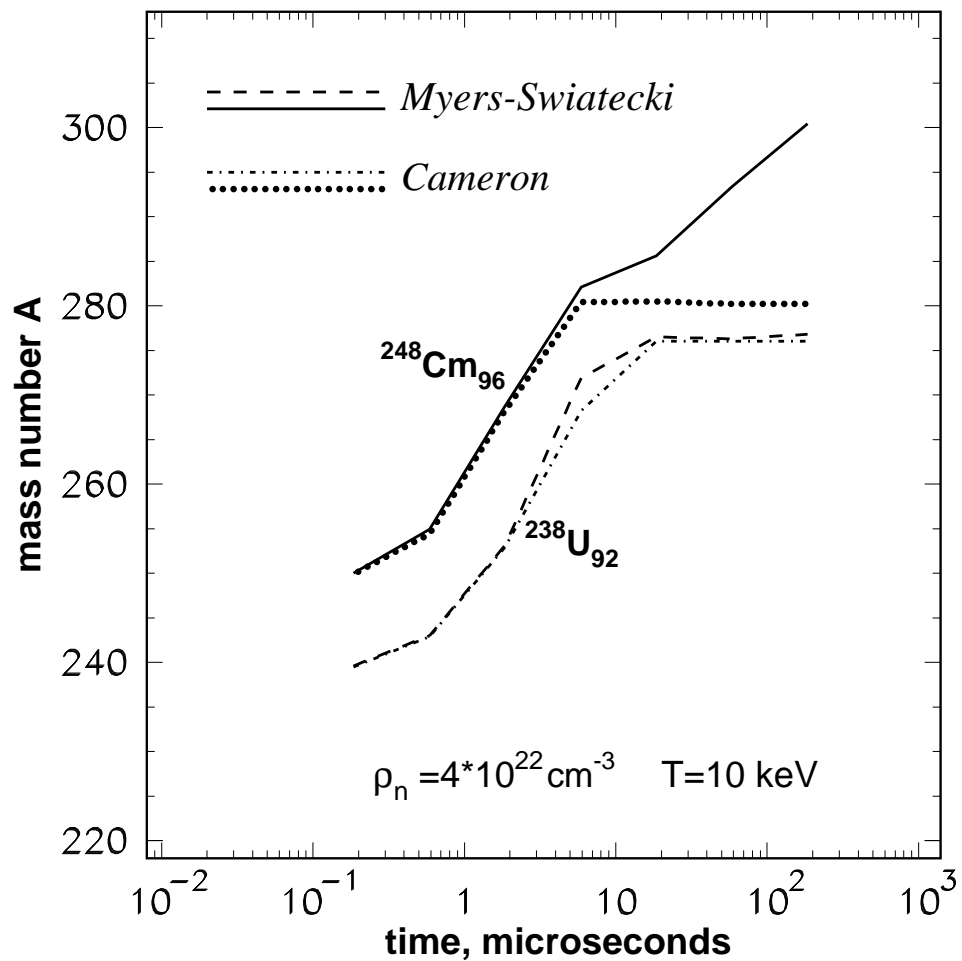


Figure 3: Effect of different mass formulae on calculations of mass number evolution for  $^{238}\text{U}$  and  $^{248}\text{Cm}$  targets. Dashed and solid lines: masses are taken from ref. [16], dotted and dash-dotted lines – ref. [19]. Neutron density, temperature are also shown in the figure.

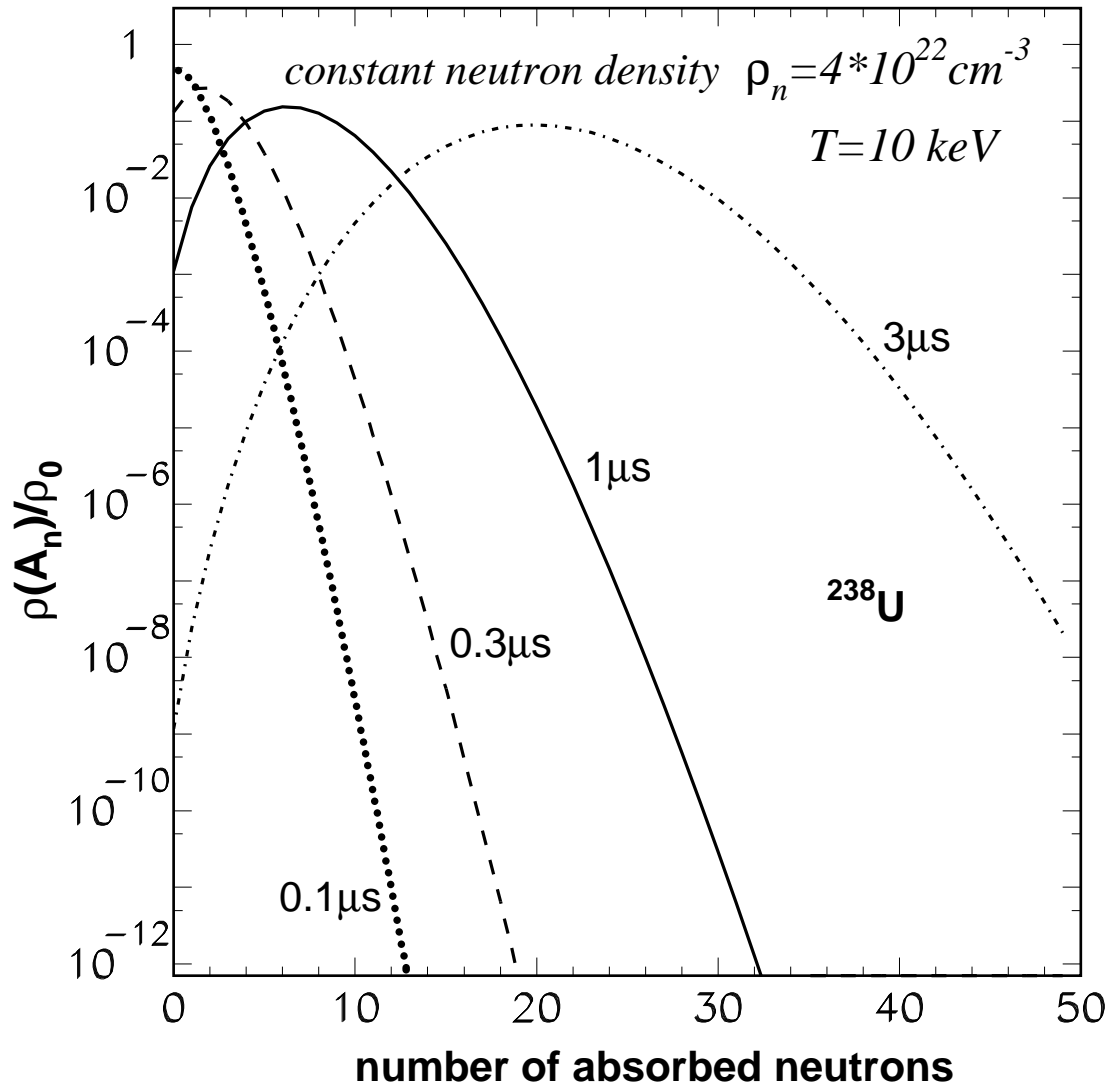


Figure 4: Densities of nuclei produced after capture of neutrons normalized to the initial density of  $^{238}\text{U}$  target. Density and temperature of neutron, as well as exposure times (in microseconds) are shown in the figure.